

# DRIP: Domain Refinement Iteration with Polytopes for Backward Reachability Analysis of Neural Feedback Loops

Michael Everett<sup>1</sup>, Rudy Bunel<sup>2</sup>, Shayegan Omidshafiei<sup>1</sup>

**Abstract**—Safety certification of data-driven control techniques remains a major open problem. This work investigates backward reachability as a framework for providing collision avoidance guarantees for systems controlled by neural network (NN) policies. Because NNs are typically not invertible, existing methods conservatively assume a domain over which to relax the NN, which causes loose over-approximations of the set of states that could lead the system into the obstacle (i.e., back-projection (BP) sets). To address this issue, we introduce DRIP, an algorithm with a refinement loop on the relaxation domain, which substantially tightens the BP set bounds. Furthermore, we introduce a formulation that enables directly obtaining closed-form representations of polytopes to bound the BP sets tighter than prior work, which required solving linear programs and using hyper-rectangles. Furthermore, this work extends the NN relaxation algorithm to handle polytope domains, which further tightens the bounds on BP sets. DRIP is demonstrated in numerical experiments on control systems, including a ground robot controlled by a learned NN obstacle avoidance policy.

## I. INTRODUCTION

Neural networks (NNs) offer promising capabilities for data-driven control of complex systems. However, formally certifying safety properties of systems that are controlled by NNs remains an open challenge in the field.

To this end, recent work developed reachability analysis techniques for Neural Feedback Loops (NFLs), i.e., dynamical systems with NN control policies [1]–[4]. For *forward* reachability analysis, these techniques compute the set of states the system could reach in the future, given an initial state set, trained NN, and dynamics model. Due to the NNs’ high dimensionality and nonlinearities, exact analysis is often intractable. Thus, current methods instead compute guaranteed over-approximations of the reachable sets, based on relaxations of the nonlinearities in the NN [1]–[3] or dynamics [1], [4]. While forward reachable sets can then be used to check whether the closed-loop system satisfies desired properties (e.g., reaching the goal), forward methods can be overly conservative for obstacle avoidance [5].

Thus, this work focuses on *backward* reachability analysis [1], [5]–[9]. The goal of backward reachability analysis is to compute backprojection (BP) sets, i.e., the set of states that will lead to a given target/obstacle set under the given NN control policy and system dynamics, as illustrated in Fig. 1. The system can be certified as safe if it starts outside the BP sets, but the non-invertibility of NNs presents a major challenge in calculating these sets. Recent work [1], [5]–[7] proposes to first compute a backreachable (BR) set, i.e., the

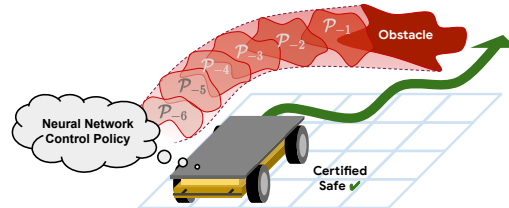


Fig. 1: Backward reachability analysis calculates the set of states ( $\mathcal{P}_{-1}, \dots, \mathcal{P}_{-6}$  in this illustration) that lead into an obstacle under a given control policy. The system is certified as safe if it starts outside those sets, without requiring any trajectory samples (green). This work develops a new algorithm for bounding these sets for NN control policies.

set of states that lead to the target set for some control input within known control limits. These methods then relax the NN controller over the BR set, which is a superset of the BP set, and calculate bounds on the BP set via linear programs.

However, a key challenge with that formulation is the BP set over-approximations can remain loose. A major cause of this conservativeness is that the BR set is often large, leading to loose NN relaxations, and thus loose BP set approximations. Moreover, conservativeness compounds when calculated over multiple timesteps due to the wrapping effect [10]. Prior work introduced strategies based on set partitioning [5]–[7] and mixed integer linear programming (MILP) [7] to improve tightness, but these methods are fundamentally hindered by initializing with the BR set. This paper instead proposes a refinement loop, which, for a particular timestep, iteratively uses the previous BP set estimate to relax the NFL and compute a new BP set, which can lead to much tighter BP set estimates. At each iteration, this new strategy shrinks the domain over which the NFL is relaxed, which leads to a less conservative relaxation and ultimately tighter bounds on the BP sets. If desired, this idea could be used in conjunction with set partitioning [5]–[7].

Another key limitation of prior work is the use of axis-aligned bounding boxes to represent BP set estimates [5]–[7]. These hyperrectangles are computed by solving several linear programs (LPs) over states and controls, but hyperrectangles are often a poor approximation of the true BP sets. Instead, this paper introduces a new approach that enables directly obtaining a closed-form polytope representation for the BP set estimate. A key reason why this enables tighter BP set bounds is that the facets of the target set (or future BP sets in the multi-timestep algorithm) can be directly used as the objective matrix for the relaxation algorithm, which also

<sup>1</sup>Google Research m.everett@northeastern.edu,omidshafiei@google.com

<sup>2</sup>DeepMind rbunel@google.com

automatically addresses the common issue of choosing facet directions in polytope design. Furthermore, we show that the NN can be relaxed over these polytope BP sets, which leads to much tighter relaxations and BP set estimates compared to prior work, which inflated polytopes to hyperrectangles.

To summarize, the main contribution of this work is DRIP, an algorithm that provides safety guarantees for NFLs, which includes domain refinement and a polytope formulation to give tighter certificates than state-of-the-art methods. Numerical experiments on the same data-driven control systems as in prior state-of-the-art works [5]–[7] demonstrate that DRIP can provide  $371\times$  tighter bounds while remaining computationally efficient ( $\sim 0.3s$ ) and can certify obstacle avoidance for a robot with a learned NN policy.

## II. BACKGROUND

This section defines the dynamics, relaxations, and sets used for backward reachability analysis.

### A. NFL Dynamics

As in [7], we assume linear time-invariant (LTI) dynamics,

$$\mathbf{x}_{t+1} = \mathbf{A}\mathbf{x}_t + \mathbf{B}\mathbf{u}_t + \mathbf{c} \triangleq f(\mathbf{x}_t, \mathbf{u}_t), \quad (1)$$

where  $\mathbf{x}_t \in \mathbb{R}^{n_x}$  is the state at discrete timestep  $t$ ,  $\mathbf{u}_t \in \mathbb{R}^{n_u}$  is the input,  $\mathbf{A} \in \mathbb{R}^{n_x \times n_x}$  and  $\mathbf{B} \in \mathbb{R}^{n_x \times n_u}$  are known system matrices, and  $\mathbf{c} \in \mathbb{R}^{n_x}$  is a known exogenous input. We assume  $\mathbf{x}_t \in \mathcal{X}$  and  $\mathbf{u}_t \in \mathcal{U}$ , where  $\mathcal{X}$  and  $\mathcal{U}$  are convex sets defining the operating region of the state space and control limits, respectively. The closed-loop dynamics are

$$\mathbf{x}_{t+1} = \mathbf{A}\mathbf{x}_t + \mathbf{B}\pi(\mathbf{x}_t) + \mathbf{c} \triangleq p(\mathbf{x}_t; \pi), \quad (2)$$

where  $\pi(\cdot)$  is a state-feedback control policy, discussed next.

### B. NN Control Policy & Relaxation

The control policy,  $\pi : \mathbb{R}^{n_x} \rightarrow \mathbb{R}^{n_u}$ , can be an arbitrary computation graph<sup>1</sup>, provided that it is composed of primitives that can be linearly relaxed [11]–[13]. That is, for each non-linearity  $\mathbf{z}_i = \sigma_i(\mathbf{z}_{i-1})$ , we need to be able to define  $\alpha_{l,i}, \beta_{l,i}, \alpha_{u,i}, \beta_{u,i}$  such that

$$\alpha_{l,i}\mathbf{z}_{i-1} + \beta_{l,i} \leq \mathbf{z}_i \leq \alpha_{u,i}\mathbf{z}_{i-1} + \beta_{u,i}. \quad (3)$$

For each primitive, values of  $\alpha_{l,i}, \beta_{l,i}, \alpha_{u,i}, \beta_{u,i}$  depend on the algorithm employed and are derived from intermediate bounds over the activation of the network, which can be obtained by applying the bound computation procedure (described next) to subsets of the network.

CROWN [14] and LIRPA algorithms in general [11] enable backward propagation of bounds (from function output to input, not to be confused with backward in time). For example, consider evaluating a lower bound on  $\mathbf{c} \cdot \mathbf{z}_i + b$ , using the relaxations defined in (3) to replace  $\mathbf{z}_i$ :

$$\begin{aligned} \min \mathbf{c} \cdot \mathbf{z}_i + b &\geq \min [\mathbf{c}]^+ (\alpha_{u,i}\mathbf{z}_{i-1} + \beta_{u,i}) \\ &\quad + [\mathbf{c}]^- (\alpha_{l,i}\mathbf{z}_{i-1} + \beta_{l,i}) + b \\ &\geq \min \left( [\mathbf{c}]^+ \alpha_{u,i} + [\mathbf{c}]^- \alpha_{l,i} \right) \mathbf{z}_{i-1} \\ &\quad + \left( [\mathbf{c}]^+ \beta_{u,i} + [\mathbf{c}]^- \beta_{l,i} + b \right), \end{aligned} \quad (4)$$

<sup>1</sup>The policies used in this work’s experiments are feedforward NNs of the form in [5]–[7] (i.e., alternating linear transformation and ReLU activation).

where  $[\mathbf{c}]^+ = \max(\mathbf{c}, 0)$  and  $[\mathbf{c}]^- = \min(\mathbf{c}, 0)$ . Through backsubstitution, we transformed a lower bound defined as a linear function over  $\mathbf{z}_i$  into a lower bound defined as a linear function over  $\mathbf{z}_{i-1}$ . By repeated application of this procedure to all operations in the network, given an objective matrix  $\mathbf{C}$  defined over the output  $\mathbf{y}$  of a computation graph,  $\mathbf{y} = g(\mathbf{x})$ , we can obtain bounds that are affine in the input  $\mathbf{x}$ :

$$\mathbf{M}\mathbf{x} + \mathbf{n} \leq \mathbf{C}\mathbf{y}. \quad (5)$$

If  $\mathbf{x}$  is within some known set  $\mathcal{X}$ , these bounds can be concretized to an actual value by solving  $\min_{\mathbf{x} \in \mathcal{X}} \mathbf{M}\mathbf{x} + \mathbf{n}$ , and closed-form solutions exist for some forms of  $\mathcal{X}$ .

Prior CROWN-based backward reachability works [5]–[7] relaxed the control policy  $\pi$ , whereas this work directly relaxes the closed-loop dynamics,  $p$ , drawing inspiration from [3], which focused on forward reachability.

### C. Backprojection Sets

Given target set,  $\mathcal{X}_T \subseteq \mathcal{X}$ , define 1- and  $t$ -step BP sets as

$$\mathcal{P}_{-1}(\mathcal{X}_T) = \{\mathbf{x} \mid p(\mathbf{x}; \pi) \in \mathcal{X}_T\} \quad (6)$$

$$\mathcal{P}_t(\mathcal{X}_T) = \{\mathbf{x} \mid p^{(-t)}(\mathbf{x}; \pi) \in \mathcal{X}_T\}, \quad (7)$$

where  $t < 0$ , and  $p^n$  is the  $n^{\text{th}}$  iterate of  $p$ , i.e.  $p^{n+1} \triangleq p \circ p^n$ . We will typically drop the argument and simply write  $\mathcal{P}_t$ .

The BP sets contain all states that will lead to the target set within some time horizon. Due to the NN control policy, computing these sets exactly is difficult. Instead, this work aims to compute BP over-approximations (BPOAs), since these over-approximations are guaranteed to also contain the true (unknown) BP sets and thus provide a conservative description of all states that will lead to the target set.

### D. Backreachable Sets & BPOAs

Next, we need a domain over which to apply the relaxation tools from Section II-B. First introduced in [1], one idea is to find the set of previous states  $\bar{\mathcal{R}}_t$  possibly leading to  $\bar{\mathcal{P}}_{t+1}$  regardless of policy, relax the neural network policy  $\pi$  over  $\bar{\mathcal{R}}_t$  into affine bounds  $\pi_t^L(\mathbf{x}_t)$  and  $\pi_t^U(\mathbf{x}_t)$ , and then derive bounds on  $\mathcal{P}_t$  from this linear relaxation. Specifically, define the set of all possible previous states, i.e., the BR set, as

$$\bar{\mathcal{R}}_t(\bar{\mathcal{P}}_{t+1}) \triangleq \{\mathbf{x} \mid \exists \mathbf{u} \in \mathcal{U} \text{ s.t. } f(\mathbf{x}, \mathbf{u}) \in \bar{\mathcal{P}}_{t+1}\}, \quad (8)$$

where  $\bar{\mathcal{P}}_0 \triangleq \mathcal{X}_T$ . Then, [5]–[7] defined a 1-step BPOA as,

$$\bar{\mathcal{P}}_{-1} \triangleq \{\mathbf{x} \mid \exists \mathbf{u} \in [\pi^L(\mathbf{x}), \pi^U(\mathbf{x})] \text{ s.t. } f(\mathbf{x}, \mathbf{u}) \in \mathcal{X}_T\}. \quad (9)$$

$\bar{\mathcal{P}}_{-1}$  is bounded by the hyper-rectangle,  $[\bar{\mathbf{x}}_{-1}, \bar{\mathbf{x}}_{-1}]$ , which requires solving the following optimization problems for each state  $k \in [n_x]$ , with the  $i$ -th standard basis vector,  $\mathbf{e}_i$ :

$$\begin{aligned} \bar{\mathbf{x}}_{-1;k} &= \min_{\mathbf{x}, \mathbf{u} \text{ s.t. } f(\mathbf{x}, \mathbf{u}) \in \mathcal{X}_T, \mathbf{u} \in [\pi^L(\mathbf{x}), \pi^U(\mathbf{x})]} \mathbf{e}_k^\top \mathbf{x} \\ \underline{\mathbf{x}}_{-1;k} &= \max_{\mathbf{x}, \mathbf{u} \text{ s.t. } f(\mathbf{x}, \mathbf{u}) \in \mathcal{X}_T, \mathbf{u} \in [\pi^L(\mathbf{x}), \pi^U(\mathbf{x})]} \mathbf{e}_k^\top \mathbf{x}. \end{aligned} \quad (10)$$

## III. APPROACH

This section introduces our proposed approach, Domain Refinement Iteration with Polytopes (DRIP), with descriptions of the 3 technical contributions in Sections III-A to III-C and a summary of the algorithm in Section III-D.

### A. Improved BP Set Representation: Polytope Formulation

Instead of relaxing  $\pi$  and solving LPs to bound  $\mathcal{P}_{-1}$ , this work instead relaxes the closed-loop dynamics,  $p(\cdot; \pi)$ , which directly results in a closed-form expression for the halfspace representation (H-rep) of the polytope BPOA. Specifically, for target set  $\mathcal{X}_T = \{\mathbf{x} \mid \mathbf{A}_T \mathbf{x} \leq \mathbf{b}_T\}$ , we apply CROWN (5) on  $p$  over the domain  $\mathcal{R}_{-1} = \{\mathbf{x} \mid \mathbf{A}_{\text{relax}} \mathbf{x} \leq \mathbf{b}_{\text{relax}}\}$  with objective  $\mathbf{C} = \mathbf{A}_T$ . This gives  $\mathbf{M}, \mathbf{n}$  such that

$$\mathbf{M}\mathbf{x}_{t-1} + \mathbf{n} \leq \mathbf{A}_T \mathbf{x}_t \quad \forall \mathbf{x}_{t-1} \in \mathcal{R}_{-1}. \quad (11)$$

Then, the set of  $\mathbf{x}_t$  that lead to  $\mathcal{X}_T$  is bounded by the constraints  $\mathbf{M}\mathbf{x}_{t-1} + \mathbf{n} \leq \mathbf{b}_T$  and  $\mathbf{x}_{t-1} \in \mathcal{R}_{-1}$ . Thus, we can write the BPOA as

$$\bar{\mathcal{P}}_{-1} = \left\{ \mathbf{x} \mid \begin{bmatrix} \mathbf{M} \\ \mathbf{A}_{\text{relax}} \end{bmatrix} \mathbf{x} \leq \begin{bmatrix} \mathbf{b}_T - \mathbf{n} \\ \mathbf{b}_{\text{relax}} \end{bmatrix} \right\}. \quad (12)$$

Whereas (10) requires solving LPs, (12) describes the BPOAs in closed form as polytopes.

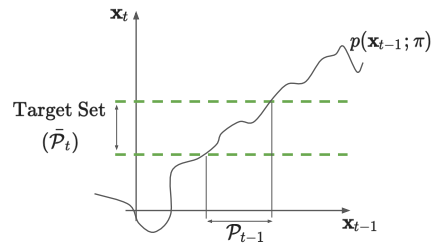
Fig. 2 illustrates this idea for a simple 1-state, 1-control system. Fig. 2a sets up the formulation: given a target set  $\mathcal{X}_T = \bar{\mathcal{P}}_t$  (green) and closed-loop dynamics  $p(\cdot; \pi)$ , the goal is to compute bounds on  $\mathcal{P}_{t-1}$  (all states at the previous timestep,  $\mathbf{x}_{t-1}$ , that lead into  $\mathcal{X}_T$  at time  $t$ ). Fig. 2b adds the BR set,  $\mathcal{R}_{t-1}$ , (red) which is calculated by solving 2 LPs (1 minimization, 1 maximization) to describe the set of  $\mathbf{x}_{t-1}$  that lead to  $\bar{\mathcal{P}}_t$  for some control within the control limits  $\mathcal{U}$ . In Fig. 2c, the closed-loop dynamics,  $p$ , are relaxed over  $\mathcal{R}_{t-1}$ , which provides bounds (blue) on the affine relationship between subsequent states,  $\mathbf{x}_{t-1}$  and  $\mathbf{x}_t$ . Finally, in Fig. 2d, define  $\bar{\mathcal{P}}_{t-1}$  based on the intersection points (magenta) of the relaxed dynamics (blue) and target set (green). The *upper* limit of  $\bar{\mathcal{P}}_{t-1}$  is the point where the *lower* bound on the closed-loop dynamics intersects with the *upper* bound of the target set, and vice versa. This formulation ensures that  $\bar{\mathcal{P}}_{t-1}$  contains only states  $\mathbf{x}_{t-1}$  for which *some* realization of the closed-loop dynamics (within the relaxation set) will lead to the target set.

More generally, the intersections in Fig. 2d might lie elsewhere or not exist. We include  $\mathcal{R}_{t-1}$  in the constraints that define  $\bar{\mathcal{P}}_{t-1}$ , both because  $\mathcal{R}_{t-1}$  is the domain over which the relaxation is valid, and to ensure  $\bar{\mathcal{P}}_{t-1}$  is closed.

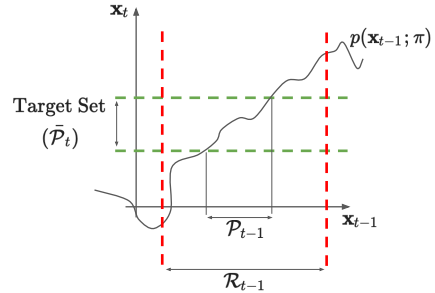
### B. Improved Relaxation Domain: Refinement Loop

While  $\mathcal{R}_{-1}$  provides a domain for relaxing the NN, this domain is often excessively conservative and leads to large BPOAs. To address this issue, this work leverages the insight that  $\mathcal{P}_{-1} \subseteq \bar{\mathcal{P}}_{-1} \subseteq \mathcal{R}_{-1}$ . In particular, after computing  $\bar{\mathcal{P}}_{-1}$  using the domain  $\mathcal{R}_{-1}$ , we can compute a new  $\bar{\mathcal{P}}'_{-1} \subseteq \bar{\mathcal{P}}_{-1}$  using the domain  $\bar{\mathcal{P}}_{-1}$ . Since  $\bar{\mathcal{P}}_{-1} \subseteq \mathcal{R}_{-1}$ , the relaxation is often tighter in practice, which can lead to a tighter BPOA. This refinement can be performed iteratively (e.g., for a specified number of steps or until the reduction in BPOA volume between refinement steps reaches some threshold).

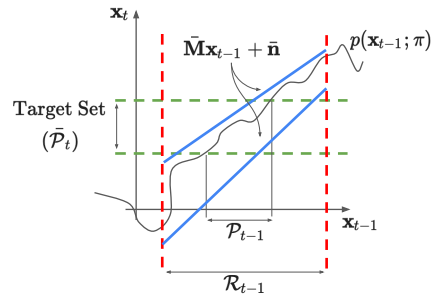
To visualize this idea, the magenta lines in Fig. 2d represent the new relaxation domain over which new affine bounds (blue) would be calculated. These new affine bounds could be much tighter, because the function's range is much smaller over this new domain.



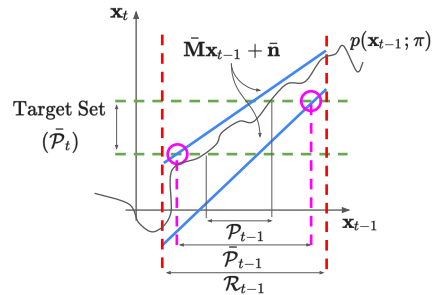
(a) Given closed-loop dynamics,  $f(\mathbf{x}_{t-1}; \pi)$  and target set,  $\bar{\mathcal{P}}_t$ , want to compute bounds on true, unknown BP set,  $\mathcal{P}_{t-1}$ .



(b) Calculate BR set,  $\mathcal{R}_{t-1}$ , using control limits,  $f$ , and  $\pi$

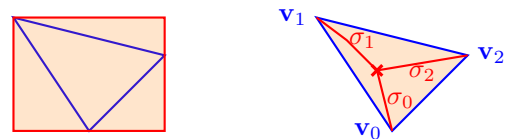


(c) Relax C.L. dynamics within  $\mathcal{R}_{t-1}$  to get affine bounds



(d) Return  $\bar{\mathcal{P}}_{t-1}$  as interval where region between affine bounds overlaps  $\bar{\mathcal{P}}_t$

Fig. 2: Method for calculating  $\bar{\mathcal{P}}_{t-1}$  from  $\bar{\mathcal{P}}_t$  using Algorithm 2. Given a target set (a), compute BR set (b), relax the closed-loop dynamics (c), to get bounds on the BP set (d).



(a) Existing work

(b) This work

Fig. 3: Comparison of how a convex polytope  $\mathcal{C}$  (blue) is handled by existing methods (a) and our method (b). The orange region denotes the domain used to relax the NN.

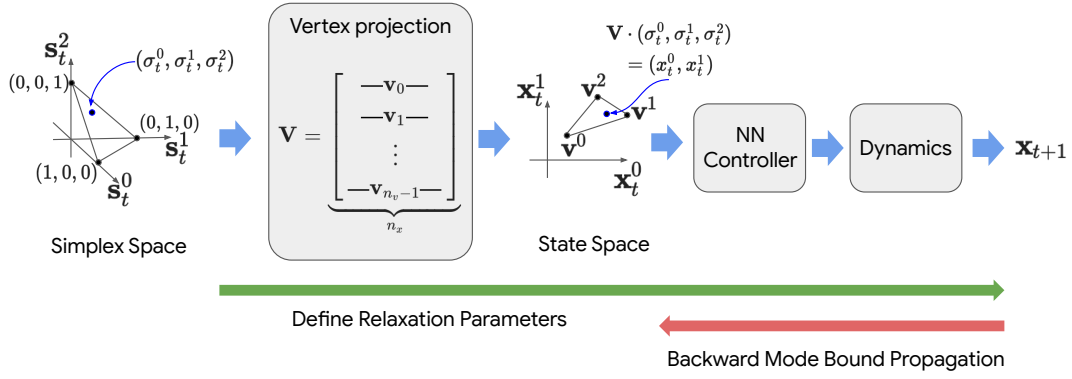


Fig. 4: Architecture to enable relaxation of closed-loop dynamics over a polytope description of the current state set. A linear transformation,  $\mathbf{V}$  (stacked polytope vertices,  $n_v = 3$  here), is added to the front of the closed-loop dynamics. This transformation projects the standard  $n_v$ -simplex onto the state space, leading to a polytope of states over which the closed-loop dynamics is relaxed. During the relaxation, the function including the vertex projection is used to define relaxation parameters, but the backward mode bound propagation stops before the vertex projection to compute  $\mathbf{M}\mathbf{x}_t + \mathbf{n} \leq \mathbf{C}\mathbf{x}_{t+1}$ .

---

#### Algorithm 1 CROWNSimplex

---

**Input:** closed-loop dynamics,  $f$ , polytope vertices  $\mathbf{V}$ , objective matrix  $\mathbf{C}$

**Output:**  $\mathbf{M}$ ,  $\mathbf{n}$ , describing affine bounds from  $\mathbf{x}_t$  to  $\mathbf{x}_{t+1}$

- 1:  $\mathbf{x}_t = \mathbf{V} \cdot \mathbf{s}$
  - 2:  $\mathbf{x}_{t+1} = f_{\text{simplex}}(\mathbf{s}) = f(\mathbf{V} \cdot \mathbf{s})$
  - 3:  $\boldsymbol{\alpha}, \boldsymbol{\beta} \leftarrow \text{defineRelaxationParams}(f_{\text{simplex}}, [\mathbf{0}_{n_v}, \mathbf{1}_{n_v}], 1)$
  - 4:  $\mathbf{M}, \mathbf{n} \leftarrow \text{bwdModeProp}(f_{\text{simplex}}, \mathbf{x}_{t+1} \rightarrow \mathbf{x}_t, \boldsymbol{\alpha}, \boldsymbol{\beta}, \mathbf{C})$
  - 5: **return**  $\mathbf{M}, \mathbf{n}$
- 

#### C. Improved Relaxation over BP Set: Polytope Input Bounds

Existing algorithms [1], [5]–[7] simplified the bound computation by assuming the domain over which to relax the network was a hyper-rectangle  $\mathcal{X} = [\mathbf{l}, \mathbf{u}]^d$ , which enables

$$\min_{\mathbf{x} \in \mathcal{X}} \mathbf{M}\mathbf{x} + \mathbf{n} = [\mathbf{M}]^+ \mathbf{l} + [\mathbf{M}]^- \mathbf{u} + \mathbf{n}. \quad (13)$$

Assuming that the input domain is a convex polytope  $\mathcal{C}$ , the strategy consists in first solving  $2d$  LPs,  $l_i = \max_{\mathbf{x} \in \mathcal{C}} x_i$  and  $u_i = \min_{\mathbf{x} \in \mathcal{C}} x_i$ , to obtain the hyperrectangle. However, this can contribute to bound conservativeness (Fig. 3a).

Instead, we propose to rely on another form of domain for which concretization of linear bounds is efficient: the simplex. If we define  $\mathcal{X} = \Delta_d = \{\mathbf{x} \in \mathcal{R}^d \mid \mathbf{x} \geq 0, \sum_i x_i = 1\}$ , then

$$\min_{\mathbf{x} \in \mathcal{X}} \mathbf{M}\mathbf{x} + \mathbf{n} = \mathbf{M}_{\text{argmin}[\mathbf{M}]} + \mathbf{n}. \quad (14)$$

We can represent a convex polytope  $\mathcal{C}$ , with a simplex and a transformation based on its vertices  $\{\mathbf{v}_0, \mathbf{v}_1, \dots, \mathbf{v}_n\}$ :

$$\mathbf{x} \in \mathcal{C} \iff \exists \boldsymbol{\sigma} \in \Delta_d \text{ such that } \mathbf{x} = \boldsymbol{\sigma} \mathbf{V}, \quad (15)$$

where  $\mathbf{V} = \text{stack}(\mathbf{v}_0, \mathbf{v}_1, \dots, \mathbf{v}_n)$ . Fig. 4 shows how this is integrated in the bound propagation: the multiplication by the matrix of vertices is simply prepended to the NN controller as an initial linear layer. As seen in Fig. 3b, this is an exact representation of polytope  $\mathcal{C}$ .

---

#### Algorithm 2 Domain Refinement with Polytopes (DRIP)

---

**Input:** target set  $\mathcal{X}_T$ , policy  $\pi$ , dynamics  $p$ , iterations  $n_{\text{iters}}$

**Output:** BP set approximation  $\bar{\mathcal{P}}_{-1}(\mathcal{X}_T)$

- 1:  $\mathbf{A}_{\mathcal{X}_T}, \mathbf{b}_{\mathcal{X}_T} \leftarrow \mathcal{X}_T = \{\mathbf{x} \mid \mathbf{A}_{\mathcal{X}_T} \mathbf{x} \leq \mathbf{b}_{\mathcal{X}_T}\}$
  - 2:  $\bar{\mathcal{P}}_{-1} \leftarrow \bar{\mathcal{R}}_{-1} = \text{backreach}(\mathcal{X}_T, \mathcal{U}, p(\cdot; \pi))$
  - 3: **for**  $i$  in  $\{1, 2, \dots, n_{\text{iters}}\}$  **do**
  - 4:  $\mathbf{V} \leftarrow \text{findVertices}(\bar{\mathcal{P}}_{-1})$
  - 5:  $\mathbf{M}, \mathbf{n} \leftarrow \text{CROWNSimplex}(p(\cdot; \pi), \mathbf{V}, \mathbf{A}_{\mathcal{X}_T})$
  - 6:  $\bar{\mathcal{P}}_{-1} \leftarrow \left\{ \mathbf{x} \mid \begin{bmatrix} \mathbf{M} \\ \mathbf{A}_{\bar{\mathcal{P}}_{-1}} \end{bmatrix} \mathbf{x} \leq \begin{bmatrix} \mathbf{b}_T - \mathbf{n} \\ \mathbf{b}_{\bar{\mathcal{P}}_{-1}} \end{bmatrix} \right\}$
  - 7: **end for**
  - 8: **return**  $\bar{\mathcal{P}}_{-1}$
- 

---

#### Algorithm 3 Multi-Step DRIP

---

**Input:** target set  $\mathcal{X}_T$ , policy  $\pi$ , dynamics  $p$ , iterations  $n_{\text{iters}}$ , time horizon  $\tau$

**Output:** BP set approximations  $\bar{\mathcal{P}}_{-\tau:0}(\mathcal{X}_T)$

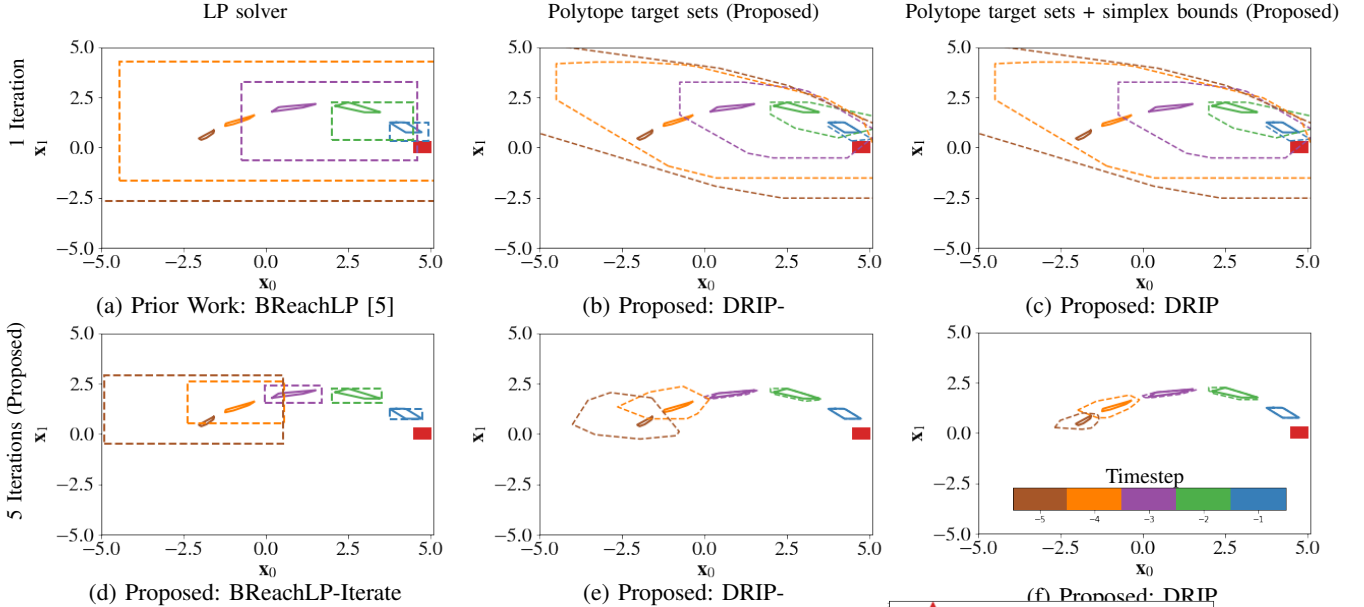
- 1:  $\bar{\mathcal{P}}_0(\mathcal{X}_T) \leftarrow \mathcal{X}_T$
  - 2: **for**  $t$  in  $\{-1, -2, \dots, -\tau\}$  **do**
  - 3:  $\bar{\mathcal{P}}_t(\mathcal{X}_T) \leftarrow \text{DRIP}(\bar{\mathcal{P}}_{t+1}(\mathcal{X}_T), \pi, p, n_{\text{iters}})$
  - 4: **end for**
  - 5: **return**  $\bar{\mathcal{P}}_{-\tau:0}(\mathcal{X}_T)$
- 

#### D. Algorithm Overview

To summarize an implementation of the proposed approach, we first describe the method for relaxing  $p$  (Algorithm 1), then show how this is used to calculate the BPOA for a single timestep (Algorithm 2), then describe how to compute BPOAs over multiple timesteps (Algorithm 3).

Given an objective matrix  $\mathbf{C} \in \mathcal{R}^{h \times n_x}$ , Algorithm 1 aims to compute  $\mathbf{M}, \mathbf{n}$  such that  $\mathbf{C}\mathbf{x}_t \leq \mathbf{M}\mathbf{x}_{t-1} + \mathbf{n} \forall \mathbf{x}_{t-1} \in \text{conv\_hull}(\mathbf{V})$ . Add a linear transformation to the front of the closed-loop dynamics to obtain a new function,  $f_{\text{simplex}} : \Delta_{n_v} \rightarrow \mathcal{X}$  (Line 2). Then, define the parameters of each relaxation  $\boldsymbol{\alpha}_{l,i}, \boldsymbol{\beta}_{l,i}, \boldsymbol{\alpha}_{u,i}, \boldsymbol{\beta}_{u,i}$ , from (3), specifying the standard  $n_v$ -simplex as the bounds on the function's input (Line 3). Finally, compute backward bounds from the objective,  $\mathbf{C}$ , to the current state,  $\mathbf{x}_t$ , stopping before

Fig. 5: Comparison of BP set bounds. Given a target set (red), proposed methods lead to much tighter bounds (dashed lines) on true BP sets (solid lines), by combining multiple iterations (bottom row), polytope target sets (middle column), and simplex bounds during relaxation (right column).



reaching the added linear transformation (Line 4).

Algorithm 2 describes the proposed method for computing a BPOA,  $\mathcal{P}_{-1}$ , which uses Algorithm 1,  $\mathcal{X}_T$  (represented as a polytope), and  $p$ . First, extract  $\mathbf{A}_T, \mathbf{b}_T$  as the H-rep of the target set polytope. Then, the BR set  $\mathcal{R}_{-1}$  is computed by solving  $2n_x$  LPs (Line 2), and the BPOA,  $\mathcal{P}_{-1}$ , is initialized as  $\mathcal{R}_{-1}$ . To refine that estimate, loop for  $n_{\text{iters}}$  (Line 3). At each iteration, compute the vertex representation (V-rep) of the current BPOA (Line 4) and run Algorithm 1 with  $\mathbf{C} = \mathbf{A}_T$  (Line 5). Then, set the parameters of the H-rep of the refined BPOA using the CROWN relaxation and target set along with the prior iteration’s BPOA. Update  $\mathcal{P}_{-1}$  and the loop continues. After  $n_{\text{iters}}$ ,  $\mathcal{P}_{-1}$  is returned.

To calculate BPOAs for a time horizon  $\tau$  into the past, Algorithm 3 simply makes  $\tau$  calls to Algorithm 2, each time using the next step’s BPOA as the target set.

#### IV. RESULTS

This section demonstrates DRIP on two simulated control systems (double integrator and mobile robot), implemented with the Jax framework [15] and `jax.verify` [13] library.

##### A. Ablation Study

Using the double integrator system and learned policy from [1], Fig. 5 demonstrates the substantial improvement in reachable set tightness enabled by our proposed method. For a target set (red)  $\mathcal{X}_T = [4.5, 5.0] \times [-0.25, 0.25]$ , the true BP sets are shown in solid colors for each timestep, and the BPOAs are shown in the same colors with dashed lines. For example, Fig. 5a implements the prior work [5], in which BPOAs become very conservative after a few timesteps. By adding the refinement loop (Section III-B), Fig. 5d shows substantial improvement with  $n_{\text{iters}} = 5$ .

However, increasing  $n_{\text{iters}} > 5$  does not improve the results with the prior LP and hyper-rectangular BPOA formulation.

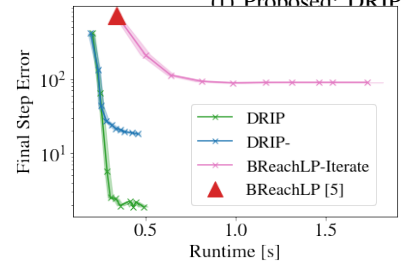


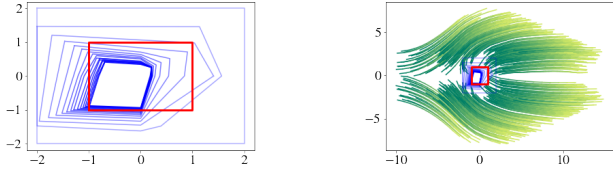
Fig. 6: Runtime vs. Error. Compared to prior work (BReachLP), the refinement loop lowers the approximation error with more computation time (BReachLP-Iterate). Incorporating target set facets reduces the error and runtime (DRIP-), and incorporating simplex bounds further improves the error with similar runtime (DRIP). Overall, there is a  $371\times$  improvement in error for similar runtime (0.3s).

Instead, the middle column shows the impact of the proposed formulation from Section III-A, in which the closed-loop dynamics are relaxed to directly provide BPOAs as polytopes. A key reason behind this improvement is the use of the target set’s facets as the objective matrix during the backward pass of the CROWN algorithm. When increasing  $n_{\text{iters}}$  to 5, we see nearly perfect bounds on the first three BP sets, with tighter yet still somewhat loose bounds on the final two timesteps.

The impact of the polytope domain used in the relaxation (Section III-C) is shown in the rightmost column. Because the first iteration always uses the hyper-rectangular  $\mathcal{R}_{-t}$ , we expect to see no difference between Fig. 5b and Fig. 5c. However, Fig. 5f shows much tighter BPOAs in the last two timesteps when compared to Fig. 5e.

Overall, the massive improvement in BPOA tightness between the prior work [5] (Fig. 5a) and the proposed approach (Fig. 5f) would enable a practitioner to certify safety when starting from a larger portion of the state space.





(a) 1-step BPOAs (blue) for 15 iterations with obstacle (red) (b) 400 rollouts with target set (red) and BPOAs (blue)

Fig. 7: Ground robot policy certification. With  $n_{\text{iters}} = 15$ ,  $\bar{\mathcal{P}}_{-1} \subseteq \mathcal{X}_T$ , which certifies that the system will never collide with the obstacle (starting anywhere outside the obstacle).

### B. Runtime vs. Error Tradeoff

Fig. 6 provides quantitative analysis of the tradeoff between tightness and computational runtime for the various methods. Final step error is the ratio  $\frac{A_{\text{BPOA}} - A_{\text{BP}}}{A_{\text{BP}}}$ , where  $A_{\mathcal{A}}$  denotes the area of set  $\mathcal{A}$ , and the runtime is plotted as the mean and shaded standard deviation over 20 trials (with the worst one discarded). For the 3 variants of the proposed algorithms, by increasing  $n_{\text{iters}}$ , we observe an improvement in error at the cost of additional runtime.

The red triangle corresponds to Fig. 5a [5]. The pink curve corresponds the leftmost column of Fig. 5, which adds a refinement loop on the relaxation domain (Section III-B). The blue curve corresponds to the middle column of Fig. 5, which uses polytope BPOAs (Section III-A). The green curve corresponds to the rightmost column of Fig. 5, which uses polytope relaxation domains (Section III-C).

A key cause of the computation time reduction between red/pink and green/blue is that the new formulation replaces many of the LPs with closed-form polytope descriptions. Overall, we observe a  $371\times$  improvement in the error. Moreover, this experiment did not require any set partitioning and was still able to provide very tight BPOAs.

### C. Ground Robot Policy Certification

Next, we use DRIP to certify that a robot will not collide with an obstacle for any initial condition in the state space (outside of the obstacle itself). We use the 2D ground robot dynamics, policy, and obstacle from [5], [7]. The target set is partitioned into 4 cells (2 per dimension), which we note is  $4\times$  fewer cells than in [5], [7]. For each cell, the 1-step BPOA is calculated for  $n_{\text{iters}}$ , and the returned BPOA is the convex hull of the union of vertices for each cell’s BPOA.

Fig. 7a shows the target set (red) and BPOA for  $n_{\text{iters}} = \{0, 1, \dots, 15\}$  (blue, darker corresponds to larger  $n_{\text{iters}}$ ). When  $n_{\text{iters}} = 15$ ,  $\bar{\mathcal{P}}_{-1} \subseteq \mathcal{X}_T$ . By Corollary A.2 of [7], this certifies that the system can only reach the obstacle if it starts from within the obstacle, and there is no need to compute BPOAs for further timesteps. Fig. 7b shows the BPOAs with rollouts of the closed-loop dynamics starting from 400 random states (green  $\rightarrow$  yellow as  $t \uparrow$ ), although sampling trajectories is not necessary given the certificate.

## V. CONCLUSION

This paper proposed a new backward reachability algorithm, DRIP, for formal safety analysis of data-driven control

systems. DRIP advances the state-of-the-art by introducing ideas to shrink the domain over which the closed-loop dynamics are relaxed and leverage polytope representations of sets at both the input and output of the relaxation. These innovations are shown to provide 2 orders of magnitude improvement in bound tightness over the prior state-of-the-art with similar runtime. Future work will investigate tighter simplex bounds [16] and convergence properties.

## REFERENCES

- [1] M. Everett, G. Habibi, C. Sun, and J. P. How, “Reachability analysis of neural feedback loops,” *IEEE Access*, vol. 9, pp. 163 938–163 953, 2021.
- [2] H. Hu, M. Fazlyab, M. Morari, and G. J. Pappas, “Reach-SDP: Reachability analysis of closed-loop systems with neural network controllers via semidefinite programming,” in *IEEE Conference on Decision and Control (CDC)*, 2020, pp. 5929–5934.
- [3] S. Chen, V. M. Preciado, and M. Fazlyab, “One-shot reachability analysis of neural network dynamical systems,” *arXiv preprint arXiv:2209.11827*, 2022.
- [4] C. Sidrane, A. Maleki, A. Irfan, and M. J. Kochenderfer, “OVERT: An algorithm for safety verification of neural network control policies for nonlinear systems,” *Journal of Machine Learning Research*, vol. 23, no. 117, pp. 1–45, 2022.
- [5] N. Rober, M. Everett, and J. P. How, “Backward reachability analysis of neural feedback loops,” in *IEEE Conference on Decision and Control (CDC)*, 2022. [Online]. Available: <https://arxiv.org/abs/2204.08319>
- [6] N. Rober, M. Everett, S. Zhang, and J. P. How, “A hybrid partitioning strategy for backward reachability of neural feedback loops,” 2023, (in review). [Online]. Available: <https://arxiv.org/abs/2210.07918>
- [7] N. Rober, S. M. Katz, C. Sidrane, E. Yel, M. Everett, M. J. Kochenderfer, and J. P. How, “Backward reachability analysis of neural feedback loops: Techniques for linear and nonlinear systems,” 2022, (in review). [Online]. Available: <https://arxiv.org/abs/2209.14076>
- [8] J. A. Vincent and M. Schwager, “Reachable polyhedral marching (RPM): A safety verification algorithm for robotic systems with deep neural network components,” in *IEEE International Conference on Robotics and Automation (ICRA)*, 2021, pp. 9029–9035.
- [9] S. Bak and H.-D. Tran, “Neural network compression of ACAS Xu early prototype is unsafe: Closed-loop verification through quantized state backreachability,” in *NASA Formal Methods*, 2022, pp. 280–298.
- [10] A. Neumaier, “The wrapping effect, ellipsoid arithmetic, stability and confidence regions,” in *Validation numerics*. Springer, 1993, pp. 175–190.
- [11] K. Xu, Z. Shi, H. Zhang, Y. Wang, K.-W. Chang, M. Huang, B. Kailkhura, X. Lin, and C.-J. Hsieh, “Automatic perturbation analysis for scalable certified robustness and beyond,” *Advances in Neural Information Processing Systems (NeurIPS)*, vol. 33, pp. 1129–1141, 2020.
- [12] S. Dathathri, K. Dvijotham, A. Kurakin, A. Raghunathan, J. Uesato, R. R. Bunel, S. Shankar, J. Steinhardt, I. Goodfellow, P. S. Liang *et al.*, “Enabling certification of verification-agnostic networks via memory-efficient semidefinite programming,” *Advances in Neural Information Processing Systems*, vol. 33, pp. 5318–5331, 2020.
- [13] DeepMind, “jax.verify,” [https://github.com/deepmind/jax\\_verify](https://github.com/deepmind/jax_verify), 2020.
- [14] H. Zhang, T.-W. Weng, P.-Y. Chen, C.-J. Hsieh, and L. Daniel, “Efficient neural network robustness certification with general activation functions,” *Advances in Neural Information Processing Systems (NeurIPS)*, 2018.
- [15] J. Bradbury, R. Frostig, P. Hawkins, M. J. Johnson, C. Leary, D. Maclaurin, G. Necula, A. Paszke, J. VanderPlas, S. Wanderman-Milne, and Q. Zhang, “JAX: composable transformations of Python+NumPy programs,” 2018. [Online]. Available: <http://github.com/google/jax>
- [16] H. S. Behl, M. P. Kumar, P. Torr, and K. Dvijotham, “Overcoming the convex barrier for simplex inputs,” *Advances in Neural Information Processing Systems*, vol. 34, pp. 4871–4882, 2021.